SEMI-ANALYTICAL FRAMEWORK FOR PRECISE RELATIVE MOTION IN LOW EARTH ORBITS

G. Gaias and C. Colombo

Department of Aerospace Science and Technology,
Politecnico di Milano, 20156 Milano, Italy

ABSTRACT

This work presents a practical and efficient semi-analytical framework for the precise modelling of the relative motion in low Earth orbits. Given the treated scenario, the orbital perturbations due to non-homogeneous Earth mass distribution and aerodynamic drag are taken into account. In accord to recent successful formation-flight experiments, the relative orbital elements parametrization is employed. And the modelling of the relative dynamics is further enhanced to take into account the effects of the whole geopotential. The paper describes the main building blocks as well as their interfaces, since the key aspect to achieve precision is to set up a fully consistent framework. Applications of the proposed tool range from the synthesis of onboard guidance navigation and control algorithms to precise relative orbit determination.

Index Terms— Formation flying, relative orbital elements, semi-analytical methods, orbital perturbations.

1. INTRODUCTION

Several multi-satellite mission architectures as formation-flying, spacecraft clusters and active debris removal require accurate modelling of the relative motion between objects in neighbouring orbits. The closer the region of interaction, the higher the level of autonomy the Guidance Navigation and Control (GNC) system may need to accomplish the mission's tasks. Hence, a precise semi-analytical framework reveals a convenient tool to support the development of efficient relative GNC algorithms. In particular, this work focuses on the Low Earth Orbits (LEO) region, with regard to applications as distributed sensors for Earth observation a/o noncooperative rendezvous to approach large pieces of debris. The customisation to the LEO environment impacts the choice of the adopted parametrization as well as the orbit perturbations to be included in the modelling.

In order to describe the relative dynamics, Orbital Elements (OEs) based approaches are often exploited (see the recent survey [1]), following the seminal works [2, 3], which recognised the advantages of linearising with respect to the OE set of the chief satellite. Generally, working in an OE space allows reducing the linearisation errors in the initial conditions, simplifies the inclusion of orbital perturbations, and allows exploiting celestial mechanics methods to identify the most efficient locations of the orbit correction manoeuvres when synthesising relative guidance and control algorithms. The state variables' set can either be constituted by differences of OE between the deputy and chief satellites or functions thereof. In both cases several OE families can be adopted, offering different levels of singularity in their definitions (e.g., classical, non-singular, equinoctial, Hoots elements) or supporting a canonical structure (e.g., Delaunay, Poincaré, Whittaker elements). Indeed the choice of which parametrization to adopt should be driven by the domain of application (singular behaviour), the conciseness/compactness of the related dynamical system, and the straightforwardness in the geometrical visualization of the relative orbits.

In view of the aforementioned design criteria, here the Relative Orbital Elements (ROEs) inherited from the co-location of geostationary satellites [4] and afterwards adapted to the formation-flying field [5] are employed. These are functions of non-singular elements that, despite their name, are singular for zero-inclinations orbits, which however have almost no practical use in the LEO region. On the other hand, in addition to the OE-based common positive characteristics, these ROEs offer the following advantages. First, ROEs merge the physical insight in the absolute orbits with a straightforward visualisation of the relative motion, as they are also trivial functions of the constants of motion of the Hill-Clohessy-Wiltshire (HCW) equations [6]. Second, there exist a direct relationship between the location of delta-v optimal manoeuvres and changes in ROEs: in-plane/out-of-plane corrections are to be executed at mean arguments of latitude corresponding to the phase angle of the total change of respectively the relative eccentricity/inclination vectors [7]. Moreover, the associated delta-v cost is proportional to the length of such total ROE change. Third, recalling their origin, ROEs allow expressing in a simple way the one-orbit minimum satellites' distance normal to the flight direction. This quantity plays a crucial role to assess the intrinsic safety of a formation, with direct exploitation into collision avoidance algorithms. For almost-bounded relative orbits, the minimum radial-normal distance is related to the phasing of the

relative eccentricity/inclination vectors [8]. Its analytical expression extended to drifting relative orbits, resulting from non-vanishing relative semi-major axis encountered during a rendezvous or produced by the action of the differential aerodynamic drag, is presented in [9].

The effectiveness of the adopted parametrization has been already demonstrated in several applications that recently flew in LEO, ranging from spaceborne GNC systems for autonomous formation keeping [10, 11], to GNC systems for spacecraft rendezvous, either ground-in-the-loop [12] or autonomous onboard [13]. This work focuses on further enhancing such framework, with key regard to *precision*. The need of improving the relative motion long-term accuracy, in fact, is for example required by angles-only initial relative orbit determination, angles-only onboard relative navigation, and long-term relative guidance policies. Above all, whenever flight data are processed, the framework consistency becomes a must to guarantee precision. When working in a pure simulation environment, where the dynamics of both satellites is propagated in the same fashion a/o observations are modelled using such simulated dynamics, in fact, the differential nature of the relative problem makes inaccuracies/inconsistencies to cancel with each other, leading to an overestimation of the *true* precision of the framework. To achieve an overall realistic accuracy one has to address specific single functions as well as their interfaces. The main building blocks, related to the aforementioned specific functions, are: the extraction of mean orbital elements, the relative dynamics including the effects of the terrestrial geopotential, and the relative dynamics subject to differential aerodynamic drag. In the sequel only the latter two aspects are explained in details. Accordingly, the main contributions of this work are the provision of a compact first-order dynamical system including the whole set of terms of the geopotential, which gives origin to a closed-form state transition matrix. Secondly, the modelling of the differential aerodynamic drag is critically discussed to show possible methods and their limitations, and to provide operational directives to use the proposed framework into realistic applications.

Focusing on the LEO environment, some functionalities of this framework exploit the assumption of small eccentricity of the chief orbit (i.e., near-circular problem). Nevertheless, some of the achieved results are actually valid for the general eccentric case, whereas others can be promptly adapted with moderate effort.

2. FRAMEWORK DEFINITION

This section introduces the structure of the framework with the support of Figure 1, where two possible sets up - propagation/guidance and navigation - are shown.

From the first outlook of Figure 1 one can note that a mixed nature of variables are involved. Recalling the advantages mentioned in the introduction, in fact, the core part of

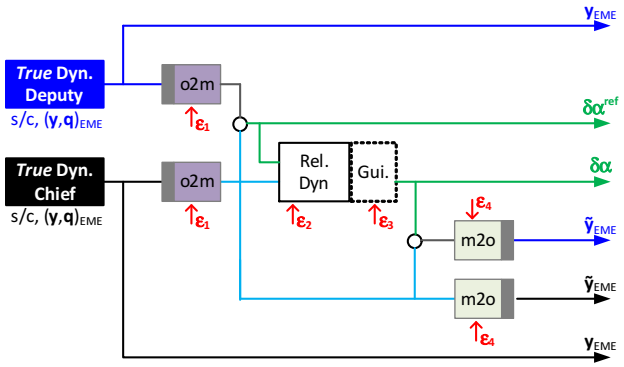

(a) Propagation/guidance set up

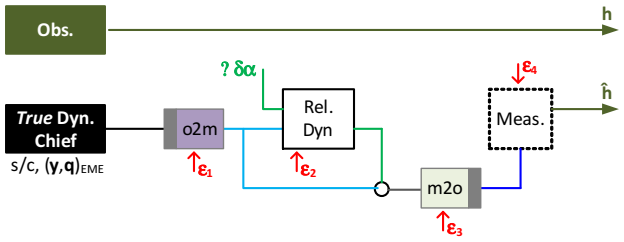

(b) Navigation set up

Fig. 1. Structure of the framework.

the relative algorithms, here represented by white-background boxes, are expressed in orbital elements (more precisely in mean OEs). At the same time, other pieces of information, like the satellites' state and the sensors' observations are conveniently expressed in Cartesian frames. In LEO, for example, the absolute orbit of a satellite is usually estimated onboard by a navigation filter that processes GPS position data. And out of such absolute navigation solution, the corresponding mean OE set has to be computed to properly interface the relative GNC algorithms. Information coming from the *true* external environment is represented by single-colour-background boxes. The remaining double-colour-background boxes identify the bridging functionalities, which link Cartesian to OE states, as well as time (i.e., synchronization) and adopted reference systems. Regarding the latter aspect, for example, estimates and observations are often expressed in the Earth Mean Equator and Equinox of J2000 (EME2000) reference system given the availability of star catalogues in that frame [14]. The osculating/mean elements conversions, instead, require a true of date (TOD) reference frame, coherently with the arrangement of the geopotential harmonics with respect to the terrestrial equator. If all these interfaces are not properly implemented, additional artificial sources of error degrade the overall accuracy of the framework. Referring to Figure 1, this can be visualised following the chain of actions that bring to $\tilde{\mathbf{y}}_{\text{EME}}$ and $\hat{\mathbf{h}}$, respectively compared to $\mathbf{y}_{\text{EME}}$ and $\mathbf{h}$. In particular, from the top-view (a) set up, the impact

of the errors in the two-way transformations (i.e., ϵ_1 and ϵ_4) can be assessed looking at the inconsistencies between $\tilde{\mathbf{y}}_{\text{EME}}$ and $\mathbf{y}_{\text{EME}}$ for the chief satellite. Moreover, ϵ_1 corrupts the initial value of the relative state (i.e., green signal input to the *Rel. Dyn.* block) prior to its propagation over time.

Recalling the introduction, the implemented framework serves several formation-flying related applications. In the propagation/guidance set up one aims at synthesising a control policy that brings the relative trajectory close to an aimed reference one (i.e., green state), minimising the inconsistency in the deputy state, to let the mission instruments operating in the most accurate conditions. In relative navigation, one estimates the relative state at a time, so that the inconsistency in the observations is minimised. This paper addresses solely the model of the relative dynamics topic; hence the errors brought by the guidance and measurement modelling blocks - highlighted with dashed borders - are not considered. The remainder of the article presents the semi-analytical modelling of the *Rel. Dyn.* box to minimise the impact of ϵ_2. Nevertheless, the accuracy obtained in the presented plots take into account a realistic ϵ_1, making the environment suitable for post-processing of real flight-data.

3. EARTH MASS DISTRIBUTION

The primary perturbation to be included in the LEO environment is the one produced by the non-homogeneous Earth mass distribution. Earth gravity models, computed from measurements and satellite observations, are released in the form of normalised gravitational coefficients up to a certain degree and order, corresponding to the spherical harmonics of the gravity potential (i.e., geopotential). Following the approach of the geometric method of [3], the relative motion problem is conveniently split into first the extraction of the elements' set with removed short- and long-periodic oscillations, second the evaluation of the relative dynamics for such mean elements' set. Coherently, these two aspects are treated hereafter.

3.1. Osculating/Mean orbital elements conversion

The computation of mean OEs is based on averaging techniques and several analytical orbital theories are given in the literature [15]. Within this framework, considering the formation flying application, the LEO scenario, and suitability for onboard implementation, an algorithm that includes a user-definable order and degree terms of the geopotential and that introduces small errors in the inverse (i.e., osculating-to-mean) transformation is used. Moreover, as the drift in the along-track direction is proportional to the relative semi-major axis, the highest precision is required only for such component of the OE set (recall the impact of ϵ_1) . As a result, the employed algorithm makes use of a second-order Lie-series based approach, closed form in eccentricity, to cancel the short- and long-periodic terms due to the dominant J_2 term from the non-singular OE set. Afterwards, the semi-major axis component only is refined through the first-order Kaula method up to the required order and degree term. The so obtained algorithm is compact, fully analytical, and non-affected by singularities.

3.2. Relative mean linearised dynamics

The relative mean motion is parametrised by the following set of dimensionless ROEs:

$$\begin{aligned} \delta\boldsymbol{\alpha} &= f(\boldsymbol{\alpha}_{\text{d}}, a_{\text{c}}, i_{\text{c}}) - f(\boldsymbol{\alpha}_{\text{c}}, a_{\text{c}}, i_{\text{c}}) \\ &= (\delta a, \delta\lambda, \delta e_x, \delta e_y, \delta i_x, \delta i_y)^{\text{T}} \end{aligned} \tag{1}$$

where

$$f(\boldsymbol{\alpha}, a_{\text{c}}, i_{\text{c}}) = (a/a_{\text{c}}, u + \Omega\cos i_{\text{c}}, e_x, e_y, i, \Omega\sin i_{\text{c}})^{\text{T}} \tag{2}$$

Here $\boldsymbol{\alpha} = (a, e, i, \Omega, \omega, u)^{\text{T}}$ is the set of classical Keplerian orbital elements, $u = \omega + M$ is the spacecraft mean argument of latitude, $e_x = e\cos\omega$, $e_y = e\sin\omega$, and the subscripts "d" and "c" denote the deputy and chief satellites. The vectors $(\delta e_x, \delta e_y)$ and $(\delta i_x, \delta i_y)$ are respectively known as the relative eccentricity and inclination vectors.

After having applied the transformations of section 3.1, the only orbital elements that vary over time are:

$$\begin{aligned} \dot{\Omega} &= \tilde{f}(a, e, i, J_2, J_2^2, J_4, J_6, ..., J_p) \\ \dot{\omega} &= \tilde{f}(a, e, i, J_2, J_2^2, J_4, J_6, ..., J_p) \\ \dot{M} &= \tilde{f}(a, e, i, J_2, J_2^2, J_4, J_6, ..., J_p) \end{aligned} \tag{3}$$

as the secular perturbations are induced by only even zonal harmonics. The $\tilde{f}$ functional expressions up to J_6 can be retrieved in [16]. Note that J_2^2, J_4, and J_6 are of the same order of magnitude, and since for the relative motion one has to regard the relative secular variations of (3), the contributions provided by terms of order greater than 6 are negligible indeed.

In order to recover the plant matrix A of the first-order relative dynamics in ROEs

$$\delta\dot{\boldsymbol{\alpha}} = A(\boldsymbol{\alpha}_{\text{c}})\,\delta\boldsymbol{\alpha} \tag{4}$$

the same approach of [17] is used. According to it,

$$\frac{d}{dt}(\delta\alpha_i) = \frac{d}{dt}\left(f_i(\boldsymbol{\alpha}_{\text{d}}) - f_i(\boldsymbol{\alpha}_{\text{c}})\right) \approx \sum_j \left.\frac{\partial g_i}{\partial\alpha_j}\right|_{\text{c}} \Delta\alpha_j \tag{5}$$

where $g_i = df_i/dt$ and the linearised expressions of $\delta\boldsymbol{\alpha}$ as function of $\Delta\boldsymbol{\alpha}$ are given by:

$$\begin{aligned} \delta a &= \Delta a/a_{\text{c}} & \delta\lambda &= \Delta u + \Delta\Omega\cos i_{\text{c}} \\ \delta i_x &= \Delta i & \delta i_y &= \Delta\Omega\sin i_{\text{c}} \end{aligned} \tag{6a}$$

$$\begin{aligned} \delta e_x &= -e_{y\text{c}}\Delta\omega + \cos\omega_{\text{c}}\Delta e \\ \delta e_y &= +e_{x\text{c}}\Delta\omega + \sin\omega_{\text{c}}\Delta e \end{aligned} \tag{6b}$$

By considering (3) and the relative state definition of (2), only the partials with respect of a, e, ω, and i for the quantities:

$$\begin{array}{rclcrcl} g_2 &=& \dot{M}+\dot{\omega}+\dot{\Omega}\cos i_\mathrm{c} & & g_3 &=& -e_y\dot{\omega} \\ g_6 &=& \dot{\Omega}\sin i_\mathrm{c} & & g_4 &=& +e_x\dot{\omega} \end{array} \tag{7}$$

need to be computed. Nevertheless, when re-arranging the equations using (6b), some terms simplify leaving only the partials with respect to a, e, and i to remain. Regarding $\dot{\Omega}$, $\dot{\omega}$, and $\dot{M}$, Tables 1 and 2 present the structures of such partials. There, $K_2 = J_2(R_\oplus/a)^2$, $K_{22} = K_2^2$, $K_4 = J_4(R_\oplus/a)^4$, $K_6 = J_6(R_\oplus/a)^6$, $R_\oplus$ is the Earth radius, $\eta = \sqrt{(1-e^2)}$, and n is the unperturbed mean motion.

Table 1. Structure of the partials for $\dot{\Omega}$ and $\dot{\omega}$

	$\frac{\partial}{\partial a}$, $\dot{\Omega}$ or $\dot{\omega}$	$\frac{\partial}{\partial e}$, $\dot{\Omega}$ or $\dot{\omega}$	$\frac{\partial}{\partial i}$, $\dot{\Omega}$ or $\dot{\omega}$
J_2	$cK_2\frac{n}{\eta^4}\frac{1}{a}f(i)$	$cK_2\frac{n}{\eta^6}ef(i)$	$cK_2\frac{n}{\eta^4}f(i)$
J_2^2	$cK_{22}\frac{n}{\eta^8}\frac{1}{a}\hat{f}$	$cK_{22}\frac{n}{\eta^{10}}e\hat{f}$	$cK_{22}\frac{n}{\eta^8}\hat{f}$
J_4	$cK_4\frac{n}{\eta^8}\frac{1}{a}\hat{f}$	$cK_4\frac{n}{\eta^{10}}e\hat{f}$	$cK_4\frac{n}{\eta^8}\hat{f}$
J_6	$cK_6\frac{n}{\eta^{12}}\frac{1}{a}\hat{f}$	$cK_6\frac{n}{\eta^{14}}e\hat{f}$	$cK_6\frac{n}{\eta^{12}}\hat{f}$

Note: c numerical coefficients, $\hat{f} = f(i, e^2)$, different for each entry.

Table 2. Structure of the partials for $\dot{M}$.

	$\frac{\partial}{\partial a}\dot{M}$	$\frac{\partial}{\partial e}\dot{M}$	$\frac{\partial}{\partial i}\dot{M}$
J_2	$cK_2\frac{n}{\eta^3}\frac{1}{a}f(i)$	$cK_2\frac{n}{\eta^5}ef(i)$	$cK_2\frac{n}{\eta^3}f(i)$
J_2^2	$cK_{22}\frac{n}{\eta^9}\frac{1}{a}\hat{f}$	$cK_{22}\frac{n}{\eta^{11}}e\hat{f}$	$cK_{22}\frac{n}{\eta^9}\hat{f}$
J_4	$cK_4\frac{n}{\eta^7}\frac{1}{a}\hat{f}$	$cK_4\frac{n}{\eta^9}e\hat{f}$	$cK_4\frac{n}{\eta^7}\hat{f}$
J_6	$cK_6\frac{n}{\eta^{11}}\frac{1}{a}\hat{f}$	$cK_6\frac{n}{\eta^{13}}e\hat{f}$	$cK_6\frac{n}{\eta^{11}}\hat{f}$

Note: c numerical coefficients, $\hat{f} = f(i, e^2)$, different for each entry.

In view of assembling the elements in the plant matrix A, the following notation is introduced:

$$\sum_p \left(\frac{\partial g_i^{(p)}}{\partial \alpha_j}\right) = G_{i,\alpha_j} \tag{8}$$

where p is the index of the ordered set $\{J_2, J_2^2, J_4, J_6\}$ collecting the considered zonal contributions. Accordingly, the non-zero terms of $A(\boldsymbol{\alpha})$ are:

$$\begin{array}{ll} A_{21} = a\,G_{2,a} & A_{61} = a\,G_{6,a} \\ A_{23} = \cos\omega\,G_{2,e} & A_{63} = \cos\omega\,G_{6,e} \\ A_{24} = \sin\omega\,G_{2,e} & A_{64} = \sin\omega\,G_{6,e} \\ A_{25} = G_{2,i} & A_{65} = G_{6,i} \\ A_{31} = a\,G_{3,a} & A_{41} = a\,G_{4,a} \\ A_{33} = \cos\omega\,G_{3,e} & A_{43} = \cos\omega\,G_{4,e} \\ A_{34} = \sin\omega\,G_{3,e} & A_{44} = \sin\omega\,G_{4,e} \\ A_{35} = G_{3,i} & A_{45} = G_{4,i} \end{array} \tag{9}$$

Therefore, the so obtained linearised system is time-variant due to the presence of sine and cosine of ω in the relative eccentricity vector lines. A linear time-invariant system can be obtained using the change of variables introduced in [18] to generalise the results of [17] to eccentric reference orbits. According to it,

$$\begin{array}{rcl} \delta\boldsymbol{\alpha}' &=& \left(\delta a, \delta\lambda, \delta e_x', \delta e_y', \delta i_x, \delta i_y\right)^\mathrm{T} \\ \delta e_x' &=& +\cos\omega\,\delta e_x + \sin\omega\,\delta e_y \\ \delta e_y' &=& -\sin\omega\,\delta e_x + \cos\omega\,\delta e_y \end{array} \tag{10}$$

and the linearised plant matrix $\tilde{A}$ for the system in the variables $\delta\boldsymbol{\alpha}'$ becomes:

$$\begin{array}{ll} \tilde{A}_{21} = a\,G_{2,a} & \tilde{A}_{61} = a\,G_{6,a} \\ \tilde{A}_{24} = G_{2,e} & \tilde{A}_{64} = G_{6,e} \\ \tilde{A}_{25} = G_{2,i} & \tilde{A}_{65} = G_{6,i} \\ \tilde{A}_{41} = a\,G_{4,a}/\cos\omega & \\ \tilde{A}_{43} = G_{4,e}/\cos\omega - \dot{\omega} & \\ \tilde{A}_{45} = G_{4,i}/\cos\omega & \end{array} \tag{11}$$

where $\cos\omega$ simplifies with the corresponding term in g_4 and $\dot{\omega}$ is function of a, e, and i only (see Table 1). Moreover, $\tilde{A}$ is nilpotent of order 2, making its exponential matrix equal to $(I + \tilde{A})$. As performed in [18], the State Transition Matrix (STM) of the original system can be computed as:

$$\Phi(\boldsymbol{\alpha}_\mathrm{c}, t_\mathrm{f}, t_0) = J^{-1}(\boldsymbol{\alpha}_\mathrm{c}(t_\mathrm{f}))\left(I + \tilde{A}(\boldsymbol{\alpha}_\mathrm{c})\right)J(\boldsymbol{\alpha}_\mathrm{c}(t_0)) \tag{12}$$

where only $\omega_\mathrm{f} = \omega_0 + \dot{\omega}(t_\mathrm{f} - t_0)$ is required at time t_f and J is the change of variables of (10). Therefore, the closed-form STM for the linearised relative motion including the geopo-

tential term till element p is expressed by:

$$\Phi_{\text{Jall}}(\boldsymbol{\alpha}_{\text{c}}, dt) = \Phi_{\text{HCW}}(\boldsymbol{\alpha}_{\text{c}}, dt) + dt \cdot \begin{bmatrix} 1 & 0 & 0 & 0 & 0 & 0 \\ aG_{2,a} & 1 & c_{\omega 0}G_{2,e} & s_{\omega 0}G_{2,e} & G_{2,i} & 0 \\ \phi_{31} & 0 & \phi_{33} & \phi_{34} & \phi_{35} & 0 \\ \phi_{41} & 0 & \phi_{43} & \phi_{44} & \phi_{45} & 0 \\ 0 & 0 & 0 & 0 & 1 & 0 \\ aG_{6,a} & 1 & c_{\omega 0}G_{6,e} & s_{\omega 0}G_{6,e} & G_{6,i} & 1 \end{bmatrix}$$

$$\begin{aligned} \phi_{31} &= -a(s_{\omega \text{f}}/c_{\omega 0})G_{4,a} \\ \phi_{33} &= +\cos(\dot{\omega}dt)/dt - e\tfrac{\partial \dot{\omega}}{\partial e}c_{\omega 0}s_{\omega \text{f}}dt \\ \phi_{34} &= -\sin(\dot{\omega}dt)/dt - e\tfrac{\partial \dot{\omega}}{\partial e}s_{\omega 0}s_{\omega \text{f}}dt \\ \phi_{35} &= -(s_{\omega \text{f}}/c_{\omega 0})G_{4,i} \\ \phi_{41} &= a(c_{\omega \text{f}}/c_{\omega 0})G_{4,a} \\ \phi_{43} &= \sin(\dot{\omega}dt)/dt + e\tfrac{\partial \dot{\omega}}{\partial e}c_{\omega 0}c_{\omega \text{f}}dt \\ \phi_{44} &= \cos(\dot{\omega}dt)/dt + e\tfrac{\partial \dot{\omega}}{\partial e}s_{\omega 0}c_{\omega \text{f}}dt \\ \phi_{45} &= (c_{\omega \text{f}}/c_{\omega 0})G_{4,i} \end{aligned} \tag{13}$$

where c_ν and s_ν respectively stand for cosine and sine of ν, $dt = t_{\text{f}} - t_0$, and Φ_{HCW} is the STM of the unperturbed problem given for example in [17]'s equation (22). Note that when neglecting terms proportional to e from (13), one finds exactly the STM used in the flight algorithms of the AVANTI (Autonomous Vision Approach Navigation and Target Identification) experiment (see equation (6) of [13]). The following comments apply to the obtained results:

1. the procedure of building A is valid for whatever order of the geopotential, even if at practical level orders greater than 6 produce negligible contributions;

2. the closed-form STM of (13) has the same validity range of the whole model (i.e., first-order), and therefore it is extremely helpful for developing onboard algorithms. In the LEO region where differential drag can be neglected (e.g., the PRISMA scenario [19, 17] at 750 km of height), equation (13) provides a fully analytical formulation precise over large periods of time, hence usable for semi-analytical relative navigation and guidance techniques;

3. if the approximation of small e can be applied (i.e., very small eccentricity a/o short time scales), it is consistent to neglect also the terms of orders greater than J_2;

4. when instead the combination of chief eccentricity and considered time scales would require a more accurate modelling, then the STM of (13) is available, with similar formal structure and properties of the simple near-circular J_2-only case. Indeed, one should properly initialise the propagation as suggested in section 3.1: errors in the initial conditions, especially in the relative semi-major axis, would nullify the improvement offered by equation (13), and therefore it would not be justified to introduce its complexity with respect to the J_2-only formulation;

5. equation (13) is valid also for the eccentric reference orbit case.

Note that first-order in the $\delta\boldsymbol{\alpha}$ variables, actually required only small δa, δe_x, δe_y, and δi_x: a similar orbit, a moderate relative semi-major axis, and no limitations in along-track direction (recall the intrinsic advantage of linearising in the OE space). This indeed is always the case for the classical domain of formation-flying, where large drifts would not be applied for operations' safety.

Figure 2 shows an example of propagation accuracy achievable when considering a 6×6 order-degree gravity potential. In this case, the chief satellite flies at 500 km of altitude with eccentricity 0.001. The initial osculating ROEs are $a\delta\boldsymbol{\alpha} = (-200.0, 4500.0, 0.0, 250.0, 0.0, 300.0)^{\text{T}}$ meters and the propagation is carried out over three days. Errors are computed with respect to the ROEs obtained integrating numerically also the deputy dynamics. The black markers identify the solution from the closed-form small-eccentricity J_2 only STM, grey markers the numerically integrated semi-analytical solution of equation (9), whereas blue dots the solution from the closed-form J-all STM of (13) (up to J_6). Note that, with a drift corresponding to 200 m of relative semi-major axis, after three days the mean along-track separation reaches 90 km (with 10 meters of accuracy). For this scenario, as the size of the relative orbit is few hundred meters, the linear model remains very precise, and the small-eccentricity assumption works very well. Indeed, the effect on the relative dynamics of the higher terms of the geopotential are providing a minor contribution; their importance appears over very large time scales. Nevertheless, to obtain such performances one has to be extremely precise in the initial mean ROEs (especially in δa). Here, in fact, to obtain such an accuracy the osculating-to-mean transformations include the all 6×6 elements, that is the same order and degree of the assumed reference dynamics.

4. DIFFERENTIAL AERODYNAMIC DRAG

The second major perturbation to be included in the LEO environment is the one produced by the differential aerodynamic drag between the deputy and the chief satellites. Differently to the geopotential case, here additional parameters have to be included to take into account the geometry of the spacecraft. In the sequel, the ballistic coefficient B is defined as $C_{\text{D}}S/m$, respectively being C_{D} the drag coefficient, S the wet area, and m the spacecraft mass. The intrinsic difficulty in modelling precisely the relative drag effects derives from the fact that the available models for atmospheric density have limited accuracy (and sometimes it is not possible to implement the most accurate ones in the onboard computer),

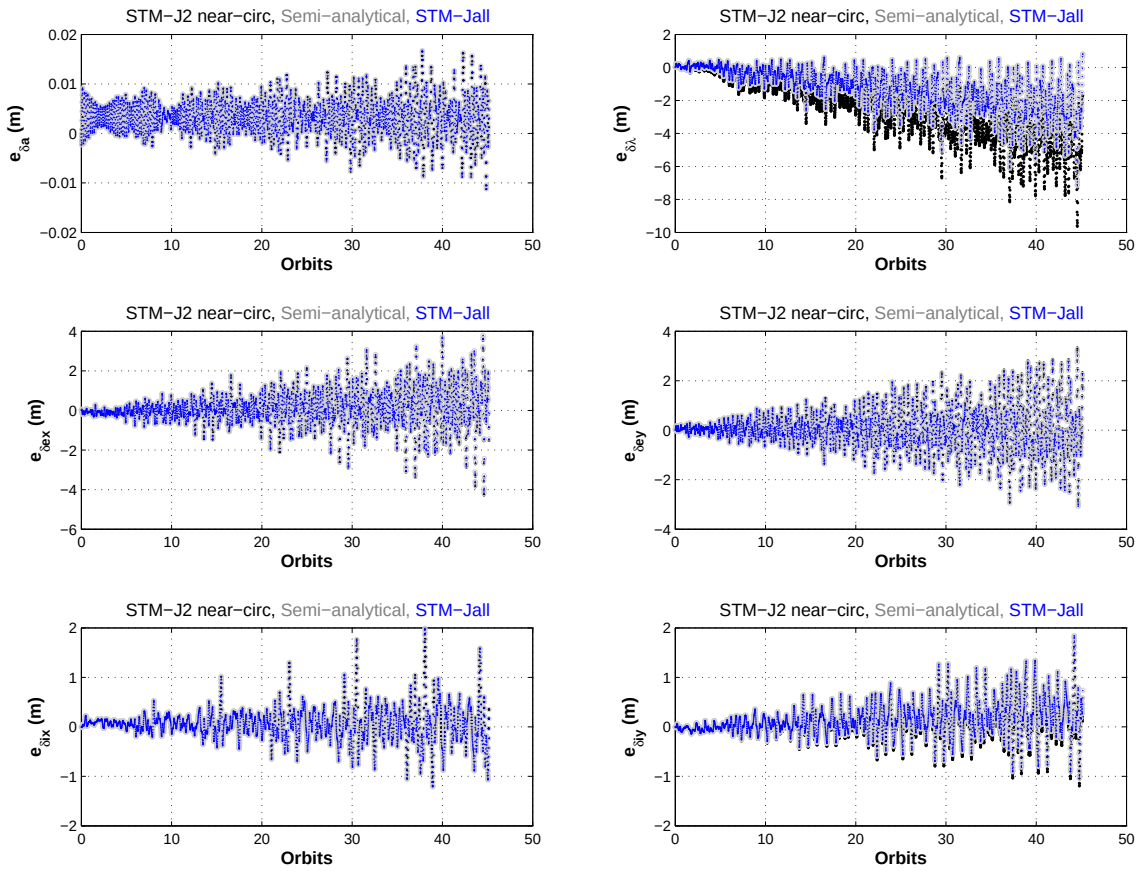

Fig. 2. Error in the relative motion modelling subject to non-homogeneous mass distribution.

the B_d of the deputy satellite is unknown for noncooperative targets, and for the chief, even if $S(t)$ may be computed depending on the current attitude, still $C_{\mathrm{D,c}}$ - function of the attitude - is not known. As a result, one has to estimate a certain amount of additional parameters out of the observations feeding the relative navigation filter. Hence, a trade-off between the number of such additional parameters and the corresponding achievable accuracy of the relative motion model has to be performed, considering that in many practical scenarios one has limited sources of observations or even weakly observable problems (i.e., angles-only relative navigation). In the literature, as for OE-based formulations only, the proposed techniques either exploit a physical approach or an engineer one. The first method directly expands the time derivatives of the averaged OEs subject to a drag acceleration with an exponential density model. Whereas the latter methodology relies on a general empirical formulation of the differential drag acceleration to include the perturbation effects produced on the ROEs. Hereafter, both are considered to complete the relative motion modelling framework developed so far.

4.1. The physical approach

This methodology has been employed by [20, 21], using the set $\boldsymbol{\xi} = (a, e, i, \Omega, \omega, M)^\mathrm{T}$ of absolute orbital elements. Under the hypothesis of considering only the tangential perturbing acceleration, ignoring in B the factor related to the atmospheric rotation, and assuming a spherical atmosphere with exponential density model, the only averaged elements varying due to the effect of drag are a and e with an average rate of [22, 16]:

$$\begin{aligned} \dot{\bar{a}} &= -B\rho_\mathrm{p} n a^2 (I_0 + 2eI_1 + \tfrac{3e^2}{4}(I_0 + I_2))e^{-z} \\ \dot{\bar{e}} &= -B\rho_\mathrm{p} n a (I_1 + \tfrac{e}{2}(I_0 + I_2) + \tfrac{e^2}{8}(5I_0 - I_3))e^{-z} \end{aligned} \tag{14}$$

Here expressions are $\mathcal{O}(e^3)$, ρ_p is the density evaluated at the perigee, and I_i are the modified Bessel functions of the first kind with argument $z = ae/H$, being H the scale height factor of the density model. By defining a relative state

$\Delta\tilde{\boldsymbol{\xi}} = (\Delta\boldsymbol{\xi}, \Delta B)^{\mathrm{T}}$, a first-order relative dynamics system can be written as:

$$\Delta\dot{\tilde{\boldsymbol{\xi}}} = A_{\mathrm{ph}}\,\Delta\tilde{\boldsymbol{\xi}} \tag{15}$$

where the components of the plant matrix related to the differential aerodynamic drag are the following:

$$\begin{array}{ll} A_{\mathrm{ph},11} = \partial\dot{\bar{a}}/\partial a & A_{\mathrm{ph},21} = \partial\dot{\bar{e}}/\partial a \\ A_{\mathrm{ph},12} = \partial\dot{\bar{a}}/\partial e & A_{\mathrm{ph},22} = \partial\dot{\bar{e}}/\partial e \\ A_{\mathrm{ph},17} = \partial\dot{\bar{a}}/\partial B & A_{\mathrm{ph},27} = \partial\dot{\bar{e}}/\partial B \end{array} \tag{16}$$

In order to merge this approach into the ROE-based formulation, one should write a plant matrix $\tilde{A}_{\mathrm{ph}}$ for the $(\delta\boldsymbol{\alpha}, \Delta B)^{\mathrm{T}}$ relative state. In this case, however, using the chain of operations (5) together with the linearised change of variables (6) introduces some errors, since the mean absolute elements that vary over time are now no more depending from the constant ones (recall Tables 1 and 2). Thus, following the steps of [22], one should start from the Gaussian form of the Lagrange variation of parameters equations in non-singular elements, write drag in the radial-tangential-normal frame, and average the change of a, e_x, and e_y. Nevertheless, the following remarks can already be done at this stage:

1. considering the inaccuracy of the exponential density model and the joint effects of drag and J_2, at least two additional parameters are to be estimated: a correction factor to ρ_{p} and the mean differential ballistic coefficient ΔB;

2. the solution of the linearised system requires always numerical integration;

3. the functional expression of the the differential aerodynamic drag acceleration is not known explicitly, but rather derived from the expansion of the averaged Gauss equations subject to $-(1/2)B\rho(\boldsymbol{\xi})v^2(\boldsymbol{\xi})$. Consequently, the introduction of further assumptions/simplifications, deriving from the specific relative scenario, is not that handy.

4.2. The engineering approach

This methodology has been proposed in [17] and it is based on the following considerations. First, the treatment of non-conservative perturbations in the linearised equations of motion in the local Cartesian frame is generally more friendly (this is especially true in the near-circular case where the equations reduce to the linear time-invariant HCW ones). Second, there is an equivalence between the linearised relative motion in the local Cartesian frame and the linearised dynamics in the OE difference parametrisation [23, 24], and thus also between (4) in ROEs. Third, the HCW equations behave like a filter with two sharp pass-bands centred on the frequencies 0 and the reciprocal of the orbital period P [25]. Thus in [17] the following general empirical formulation is proposed to express the differential aerodynamic drag acceleration acting in the local tangential (T) direction:

$$a_{\Delta\mathrm{D}}^{(\mathrm{T})} = c_1 + c_2 \sin\left(\frac{2\pi}{P}t\right) + c_3 \cos\left(\frac{2\pi}{P}t\right) \tag{17}$$

By mapping the solution of the HCW equations forced by (17) in the ROE space, the following relationship between the additional parameters c_i and the ROEs is derived:

$$a\delta\dot{a} = \tfrac{2}{n}c_1 \quad a\delta\dot{e}_x = \tfrac{1}{n}c_2 \quad a\delta\dot{e}_y = \tfrac{1}{n}c_3 \tag{18}$$

Alternatively, here we show that the same result can be achieved by using the change of variables introduced by [26] to express the in-plane motion with respect to the average position $(\bar{x}, \bar{y})$ in the local radial (R), tangential (T) plane:

$$\begin{array}{l} \mathbf{x} = (x, \dot{x}, y, \dot{y})^{\mathrm{T}} \mapsto \boldsymbol{\kappa} = (\bar{x}, \bar{y}, \gamma, \beta)^{\mathrm{T}} \\ \gamma = x - \bar{x}, \qquad \bar{x} = 4x + 2\dot{y}/n \\ \beta = y - \bar{y}, \qquad \bar{y} = y - 2\dot{x}/n \end{array} \tag{19}$$

As explained in [26], since

$$\gamma = -\frac{1}{2n}\dot{\beta} \qquad \bar{x} = -\frac{2}{3n}\dot{\bar{y}} \tag{20}$$

the HCW equations in the new variables $(\bar{y}, \beta)$ become two decoupled second order differential equations, respectively a double-integrator and an harmonic oscillator. Therefore, the inclusion of the empirical acceleration of (17), is equivalent to solve:

$$\begin{cases} \ddot{\bar{y}} = -3a_{\Delta\mathrm{D}}^{(\mathrm{T})} \\ \ddot{\beta} + n^2\beta = 4a_{\Delta\mathrm{D}}^{(\mathrm{T})} \end{cases} \tag{21}$$

As ROEs are related to the integration constants of the HCW [6], the following relationship between $\boldsymbol{\kappa}$ and the in-plane ROEs $\delta\boldsymbol{\alpha}^{\mathrm{ip}}$ exists:

$$\begin{array}{l} a(\delta a_0, \delta\lambda_0, \delta e_{x0}, \delta e_{y0})^{\mathrm{T}} = (\bar{x}_0, \bar{y}_0, -\gamma_0, -\beta_0/2)^{\mathrm{T}} \\ a\delta\boldsymbol{\alpha}^{\mathrm{ip}}(t) = M\boldsymbol{\kappa}(t) \\ M = \begin{bmatrix} 1 & 0 & 0 & 0 \\ 0 & 1 & 0 & 0 \\ 0 & 0 & -\cos(nt) & +\sin(nt)/2 \\ 0 & 0 & -\sin(nt) & -\cos(nt)/2 \end{bmatrix} \end{array} \tag{22}$$

Thus, the solution of (21), using (20) and (22) can be expressed in ROEs to obtain the equations (28)-(30) of [17], leading to (18), in a more compact way.

The differential aerodynamic drag expressed in the local RTN frame centred on the chief satellite is:

$$\begin{array}{rcl} \mathbf{a}_{\Delta\mathrm{D}}^{(\mathrm{RTN,c})} & = & R_{\mathrm{RTN,d}}^{\mathrm{RTN,c}} R_{\mathrm{TOD}}^{\mathrm{RTN,d}} \mathbf{a}_{\mathrm{D,d}}^{(\mathrm{TOD})} - R_{\mathrm{TOD}}^{\mathrm{RTN,c}} \mathbf{a}_{\mathrm{D,c}}^{(\mathrm{TOD})} \\ \mathbf{a}_{\mathrm{D}}^{(\mathrm{TOD})} & = & -\frac{1}{2}\rho B \left\|\mathbf{v} - \mathbf{v}_{\mathrm{atm}}\right\| (\mathbf{v} - \mathbf{v}_{\mathrm{atm}}) \end{array} \tag{23}$$

where the TOD frame is the inertial reference frame coherent with section 2. In the relative sense, one can indeed neglect

the effect of the velocity of the atmosphere and of the difference in local frames. Moreover, the radial and normal components are two order of magnitude smaller than the tangential one. Thus, the empirical expression (17) is the trigonometric approximation of:

$$a_{\Delta\mathrm{D}}^{(\mathrm{T})} = -(1/2)\rho_{\mathrm{d}} B_{\mathrm{d}} v_{\mathrm{d}}^2 + (1/2)\rho_{\mathrm{c}} B_{\mathrm{c}} v_{\mathrm{c}}^2 \tag{24}$$

In addition, whenever the satellites are separated by few tens of kilometres, this further simplification becomes realistic:

$$a_{\Delta\mathrm{D}}^{(\mathrm{T})} = -(1/2)\rho_{\mathrm{c}} v_{\mathrm{c}}^2 (\bar{B}_{\mathrm{d}} - \bar{B}_{\mathrm{c}}(1+b)) \tag{25}$$

i.e., the satellites have almost same absolute velocity and experience almost same density. Note that in (25) the terms varying over time are ρ_{c}, v_{c}, and b, where the latter is the zero-mean varying ballistic coefficient of the chief satellite due to its attitude profile. Being the attitude a/o the geometry of the deputy spacecraft generally not known, it is reasonable to estimate its mean ballistic coefficient only. At this stage the following remarks apply:

1. this formulation requires at most three additional parameters, which have the physical meaning of mean secular variation of δa, δe_x, and δe_y due to differential drag. These coefficients are able to catch the combined effects of all time varying quantities, comprised density day/night variations and time-varying ballistic coefficients;

2. if enough observations are available, $\delta\dot{a}$, $\delta\dot{e}_x$, and $\delta\dot{e}_y$ can be estimated by fitting their mean trend to the net of the changes caused by the geopotential, known from (13);

3. if a good model of the differential aerodynamic drag is known/available, the coefficients c_i can be computed through its fast Fourier transform (i.e., trigonometric interpolation). In particular, when the employed density model is accurate enough, one can use the convenient approximation of (25);

4. if only one additional parameter can be estimated by the filter, than $\delta\dot{a}$ is to be chosen. It catches in a density-model-free way the mean effect due to $\rho v^2 \Delta\bar{B}$. Thus, this achieves the same result of the physical approach requiring one additional parameter less. The remaining error in the relative eccentricity vector is proportional to the relevance of the neglected time-varying effects (e.g., $\rho(t)$ and $b(t)$).

In view of the aforementioned considerations, the framework is completed using the engineering approach, to obtained the following closed-form STM for the first-order relative dynamics subject to joint geopotential and differential drag:

$$\delta\hat{\boldsymbol{\alpha}}(t_0+dt) = \hat{\Phi}(\boldsymbol{\alpha}_{\mathrm{c}0}, dt)\, \delta\hat{\boldsymbol{\alpha}}(t_0)$$

$$\hat{\Phi}(\boldsymbol{\alpha}_{\mathrm{c}0}, dt) = \begin{bmatrix} \Phi_{\text{Jall}} & \Phi_{\Delta\mathrm{D}} \\ O_{3\text{x}6} & I_{3\text{x}3} \end{bmatrix}$$

$$\begin{aligned}
\phi_{\text{d-drag }11} &= dt \\
\phi_{\text{d-drag }12} &= \tfrac{2}{n}\sin(u_{\mathrm{f}} - u_0) \\
\phi_{\text{d-drag }13} &= \tfrac{2}{n}(1 - \cos(u_{\mathrm{f}} - u_0)) \\
\phi_{\text{d-drag }21} &= -\tfrac{3}{4} n dt^2 + \tfrac{1}{2} a_0 G_{2,a} dt^2 \\
\phi_{\text{d-drag }22} &= -\tfrac{3}{n}(1 - \cos(u_{\mathrm{f}} - u_0)) \\
\phi_{\text{d-drag }23} &= -3dt + \tfrac{3}{n}\sin(u_{\mathrm{f}} - u_0) \\
\phi_{\text{d-drag }31} &= \tfrac{1}{n}\sin(u_{\mathrm{f}} - u_0) \\
\phi_{\text{d-drag }32} &= dt + \tfrac{1}{n}\sin(u_{\mathrm{f}} - u_0)\cos(u_{\mathrm{f}} - u_0) \\
\phi_{\text{d-drag }33} &= \tfrac{1}{n}\sin^2(u_{\mathrm{f}} - u_0) \\
\phi_{\text{d-drag }41} &= \tfrac{1}{n}(1 - \cos(u_{\mathrm{f}} - u_0)) \\
\phi_{\text{d-drag }42} &= \tfrac{1}{n}\sin^2(u_{\mathrm{f}} - u_0) \\
\phi_{\text{d-drag }32} &= dt - \tfrac{1}{n}\sin(u_{\mathrm{f}} - u_0)\cos(u_{\mathrm{f}} - u_0) \\
\phi_{\text{d-drag }61} &= \tfrac{1}{2} a_0 G_{6,a} dt^2
\end{aligned} \tag{26}$$

Figure 3 shows an example of propagation accuracy achievable when considering a 6×6 order-degree gravity potential and the effect of differential drag. In the *true* dynamics, the Jacchia 71 model is used to compute the density values, and the spacecraft are customised on the AVANTI scenario [13]. The chief moves on the same orbit of the example of Figure 2, whereas now the initial δa is zero: the drift is created by the effect of differential drag only. Propagation is carried out over one day: considering the domain of investigation, the practical difficulties in estimating the drag effects, and the building up of relative drift, it is reasonable to consider a greater frequency of orbit correction manoeuvres (i.e., shorter manoeuvre free propagation legs). In Figure 3 the solution from the closed-form STM of (26) is shown: black markers are obtained when only $\delta\dot{a}$ is considered, whereas blue dots take into account also the estimated values of $(\delta\dot{e}_x, \delta\dot{e}_y)$. For this scenario, a very accurate result is obtained, as the additional parameters could be numerically fitted. Thus, this provides the potential best accuracy this modelling can provide. Note that in this case the effect of the sub-modelling of the relative eccentricity vector behaviour is pretty small, since the *true* dynamics is not including variation of the wet areas (related to the attitude profile) a/o uncertainty in the drag coefficients. On the other hand, the adopted formulation provides a practical tool to get a quantitative insight of the effects on the relative orbit produced by unknown factors.

5. CONCLUSION

This work presented a semi-analytical framework for the precise modelling of the relative motion in the low Earth orbit

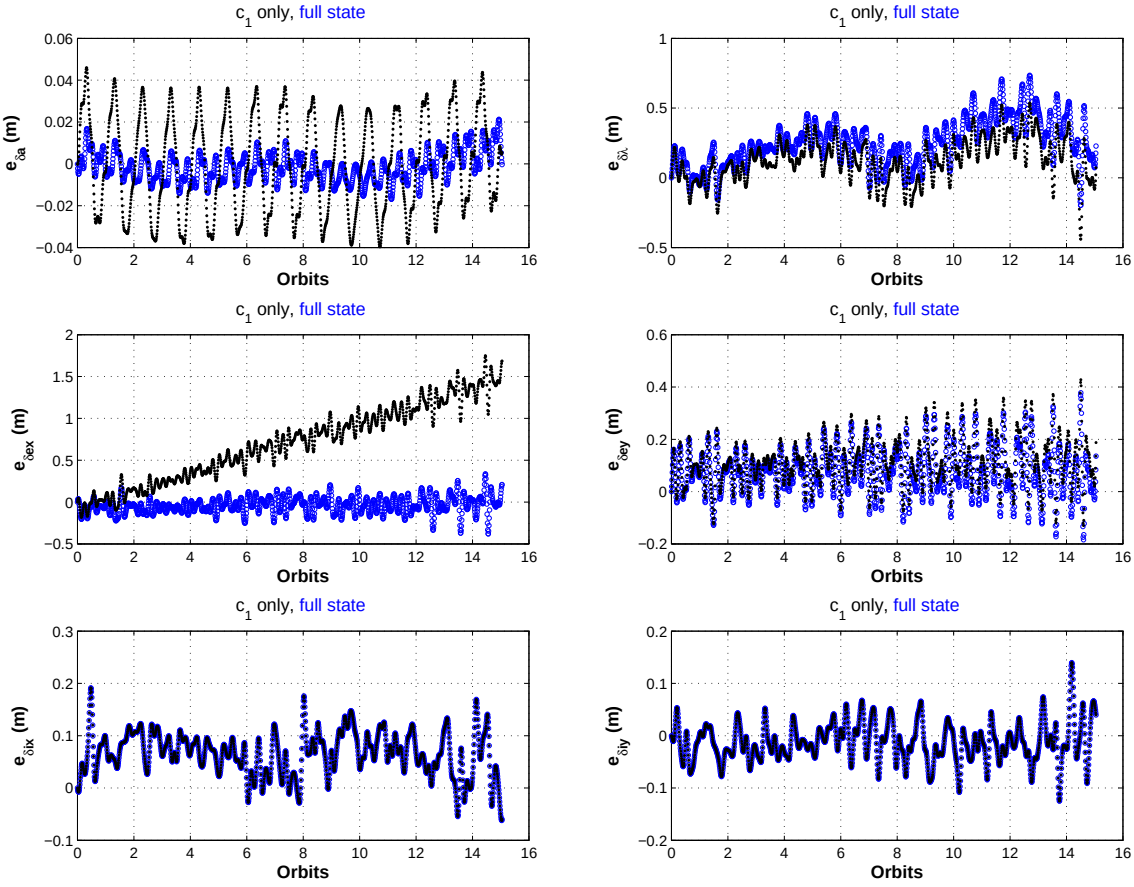

Fig. 3. Error in the relative motion modelling subject to non-homogeneous mass distribution and differential drag perturbations. The estimated additional parameters of (18) respectively amount to $-5.981e-4$, $-1.73e-5$, and $-6.06e-7$ m/s.

environment, parametrised in relative orbital elements. The paper described main functions, their interfaces, achievable performances, and practical guidelines to employ it for relative guidance navigation and control applications.

6. ACKNOWLEDGEMENTS

This project has received funding from the European Research Council (ERC) under the European Union's Horizon 2020 research and innovation programme (grant agreement No 679086 - COMPASS).

7. REFERENCES

[1] Joshua Sullivan, Sebastian Grimberg, and Simone D'Amico, "Comprehensive Survey and Assessment of Spacecraft Relative Motion Dynamics Models," *Journal of Guidance, Control, and Dynamics*, vol. 40, no. 8, pp. 1837–1859, 2017, doi: 10.2514/1.G002309.

[2] H. Schaub, S. R. Vadali, and K. T. Alfriend, "Spacecraft formation flying control using mean orbit elements," *Journal of the Astronautical Sciences*, vol. 48, no. 1, pp. 69–87, 2000.

[3] Dong-Woo Gim and Kyle T. Alfriend, "State Transition Matrix of Relative Motion for the Perturbed Noncircular Reference Orbit," *Journal of Guidance, Control, and Dynamics*, vol. 26, no. 6, pp. 956–971, 2003.

[4] A. Härting, C. K. Rajasingh, M. C. Eckstein, A. F. Leibold, and K. N. Srinivasamurthy, "On the collision hazard of colocated geostationary satellites," Minneapolis, USA, 1988, AIAA/AAS Astrodynamics conference, number 88-4239.

[5] Simone D'Amico, *Autonomous Formation Flying in*

Low Earth Orbit, Ph.D. thesis, Technical University of Delft, The Netherlands, Mar. 2010.

[6] S. D'Amico, "Relative Orbital Elements as Integration Constants of Hill's Equations," DLR-GSOC TN 05-08, Deutsches Zentrum für Luft- und Raumfahrt, Oberpfaffenhofen, Germany, Dec. 2005.

[7] Gabriella Gaias and Simone D'Amico, "Impulsive Maneuvers for Formation Reconfiguration using Relative Orbital Elements," *Journal of Guidance, Control, and Dynamics*, vol. 38, no. 6, pp. 1036–1049, 2015, doi: 10.2514/1.G000191.

[8] O. Montenbruck, M. Kirschner, S. D'Amico, and S. Bettadpur, "E/I-Vector Separation for Safe Switching of the GRACE Formation," *Aerospace Science and Technology*, vol. 10, no. 7, pp. 628–635, 2006, doi: 10.1016/j.ast.2006.04.001.

[9] G. Gaias and J.-S. Ardaens, "Design challenges and safety concept for the avanti experiment," *Acta Astronautica*, vol. 123, pp. 409–419, 2016, doi: 10.1016/j.actaastro.2015.12.034.

[10] S. D'Amico, J.-S. Ardaens, and R. Larsson, "Spaceborne Autonomous Formation-Flying Experiment on the PRISMA Mission," *Journal of Guidance, Control, and Dynamics*, vol. 35, no. 3, pp. 834–850, 2012, doi: 10.2514/1.55638.

[11] J.-S. Ardaens, S. D'Amico, and D. Fischer, "Early Flight Results from the TanDEM-X Autonomous Formation Flying System," in *Proceedings of the 4th International Conference on Spacecraft Formation Flying Missions & Technologies (SFFMT)*, St-Hubert, Quebec, 2011, Canadian Space Agency.

[12] S. D'Amico, J.-S. Ardaens, G. Gaias, H. Benninghoff, B. Schlepp, and J. L. Jørgensen, "Noncooperative Rendezvous Using Angles-Only Optical Navigation: System Design and Flight Results," *Journal of Guidance, Control, and Dynamics*, vol. 36, no. 6, pp. 1576–1595, 2013, doi: 10.2514/1.59236.

[13] Gabriella Gaias and Jean-Sébastien Ardaens, "Flight Demonstration of Autonomous Noncooperative Rendezvous in Low Earth Orbit," *Journal of Guidance, Control, and Dynamics*, vol. 41, no. 6, pp. 1337–1354, 2018.

[14] Oliver Montenbruck and Eberhard Gill, *Satellite Orbits - Models, Methods, and Applications*, Springer Verlag, 2001.

[15] Edwin Wnuk, "Recent Progress in Analytical Orbit Theories," *Advances in Space Research*, vol. 23, no. 4, pp. 677–687, 1999, doi: 10.1016/S0273-1177(99)00148-9.

[16] L. Blitzer, *Handbook of Orbital Perturbations*, Univ. of Arizona Press, Tucson, AZ, 1970.

[17] G. Gaias, J.-S. Ardaens, and O. Montenbruck, "Model of J2 Perturbed Satellite Relative Motion with Time-Varying Differential Drag," *Celestial Mechanics and Dynamical Astronomy*, vol. 123, no. 4, pp. 411–433, 2015, doi: 10.1007/s10569-015-9643-2.

[18] Adam W. Koenig, Tommaso Guffanti, and Simone D'Amico, "New State Transition Matrices for Spacecraft Relative Motion in Perturbed Orbits," *Journal of Guidance, Control, and Dynamics*, vol. 40, no. 7, pp. 1749–1768, 2017, doi: 10.2514/1.G002409.

[19] P. Bodin, R. Noteborn, R. Larsson, T. Karlsson, S. D'Amico, J.-S. Ardaens, M. Delpech, and J.-C. Berges, "PRISMA Formation Flying Demonstrator: Overview and Conclusions from the Nominal Mission," Breckenridge, Colorado, USA, 2012, 35th Annual AAS Guidance and Control Conference, number 12-072.

[20] D. Mishne, "Formation Control of Satellites Subject to Drag Variations and J_2 Perturbations," *Journal of Guidance, Control and Dynamics*, vol. 27, no. 4, pp. 685–692, 2004.

[21] O. Ben-Yaacov and P. Gurfil, "Long-Term Cluster Flight of Multiple Satellites Using Differential Drag," *Journal of Guidance, Control, and Dynamics*, vol. 36, no. 6, pp. 1731–1740, 2013, doi: 10.2514/1.61496.

[22] D. King-Hele, *Theory of satellite orbits in an atmosphere*, London Butterworths, 1964.

[23] P. Sengupta and S. R. Vadali, "Relative Motion and the Geometry of Formations in Keplerian Elliptic Orbits with Arbitrary Eccentricity," *Journal of Guidance, Control, and Dynamics*, vol. 30, no. 4, pp. 953–964, 2007, doi: 10.2514/1.25941.

[24] Andrew J. Sinclair, Ryan E. Sherrill, and T. Alan Lovell, "Calibration of Linearized Solutions for Satellite Relative Motion," *Journal of Guidance, Control, and Dynamics*, vol. 37, no. 4, pp. 1362–1367, 2014, doi: 10.2514/1.G000037.

[25] Oscar L. Colombo, "The dynamics of global position system orbits and the determination of precise ephemerides," *Journal of Geophysical Research*, vol. 94, pp. 9167–9182, 1989.

[26] C. L. Leonard, W. M. Hollister, and E. V. Bergmann, "Orbital Formationkeeping with Differential Drag," *Journal of Guidance, Control, and Dynamics*, vol. 12, no. 1, pp. 108–113, 1989, doi: 10.2514/3.20374.